

**VNIR MULTISPECTRAL OBSERVATIONS OF ROCKS AT SPIRIT OF ST. LOUIS CRATER AND MARATHON VALLEY ON THE RIM OF ENDEAVOUR CRATER MADE BY THE OPPORTUNITY ROVER PANCAM.** W.H. Farrand<sup>1</sup>, J.R. Johnson<sup>2</sup>, J.F. Bell III<sup>3</sup>, D.W. Mittlefehldt<sup>4</sup>. <sup>1</sup>Space Science Institute, 4750 Walnut St., #205, Boulder, CO 80301, farrand@spacescience.org, <sup>2</sup>Applied Physics Lab, Johns Hopkins University, Laurel, MD. <sup>3</sup>Arizona State University, Tempe, AZ, <sup>4</sup>NASA Johnson Space Center, Houston, TX.

**Introduction:** The Mars Exploration Rover Opportunity has been exploring the western rim of the 22 km diameter Endeavour crater since August, 2011 [1,2]. Recently, Opportunity has reached a break in the Endeavour rim that the rover team has named Marathon Valley. This is the site where orbital observations from the MRO CRISM imaging spectrometer indicated the presence of Fe smectites. On the outer western portion of Marathon Valley, Opportunity explored the crater-form feature dubbed Spirit of St. Louis (SoSL) crater. This presentation describes the 430 to 1009 nm (VNIR) reflectance, measured by the rover’s Pancam, of rock units present both at Spirit of St. Louis and within Marathon Valley.

**VNIR Spectral Processing:** Full spectral coverage of rock targets consists of 13 filter (13f) data collections with 11 spectrally unique channels [3]. 55 Pancam 13f data collections in the SoSL to Marathon Valley areas were characterized in terms of spectral parameters summarized in **Table 1** (discussed in more detail in [4,5]). Associations between these spectra were quantified through the use of a Kohonen-type self-organizing map (SOM) [6,7] wherein the spectral parameters listed in **Table 1** from the 55 spectra were input to the SOM and organized with similar spectral features being grouped more closely on the resulting two dimensional “map” representation. The SOM consists of 5x5 nodes wherein like observations were grouped within the same, or adjacent nodes. Each node has a representative signature and data points are mapped to the appropriate node.

**Table 1.** Spectral Parameters used in Pancam analysis

Parameter	Utility
482 to 673 nm Slope	Nanophase Fe <sup>3+</sup> oxides
535 nm Band Depth	Crystalline Fe <sup>3+</sup> oxides
601 nm Band Depth	Relative degree of oxidation
800/904 nm	Strength of Fe <sup>3+</sup> or Fe <sup>2+</sup> band
904 nm Band Depth	Strength of Fe <sup>3+</sup> or Fe <sup>2+</sup> band
754 to 1009 nm slope	Presence of Fe <sup>3+</sup> oxides
934 to 1009 nm slope	Indicator of H <sub>2</sub> O overtone
Reflectance max. posn.	Influenced by width of Fe band

**Results:** The SOM map created using the spectral parameters (**Table 1**) is shown in **Fig. 1** as a fan diagram, where higher values of a parameter are represented by a longer radius slice within each node. App-

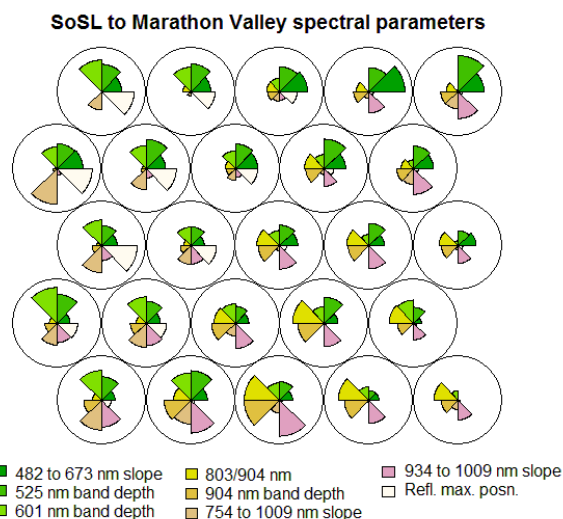


**Fig. 1.** SOM of relative strengths of spectral parameters in each node of the 5x5 SOM.

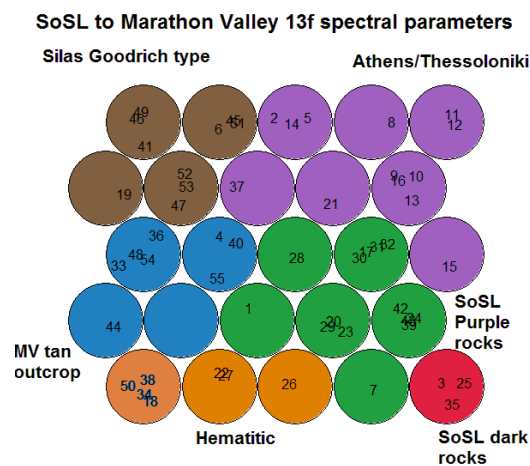


**Fig. 2.** Clustering applied to SOM. Numbers represent spectrum number.

lication of hierarchical clustering to the signatures associated with each node resulted in the six color-coded groupings shown in **Fig. 2**. As noted above the predicted signature for each node might not actually correspond to any data points (hence one blank node in **Fig. 2**). These six groupings are: 1) Pvt. Silas Goodrich type spectra, 2) Marathon Valley tan outcrop, 3) Athens/Thessaloniki, 4) hematitic rocks, 5) SoSL purple rocks, and 6) SoSL dark rocks. Representative spectra from these groupings are shown in **Fig. 3** and images

of the rocks are shown in **Fig. 4**. These groupings are characterized by: 1) long wavelength reflectance peak position, convex NIR shape, negative 934 to 1009 nm slope; 2) positive 601 nm band depth; 3) high 535 nm band depth, highly negative 601 nm band depth; 4) strong 904 nm band, positive 934 to 1009 nm slope; 5 and 6) relatively low 535 nm band depth and reflectance peak position.

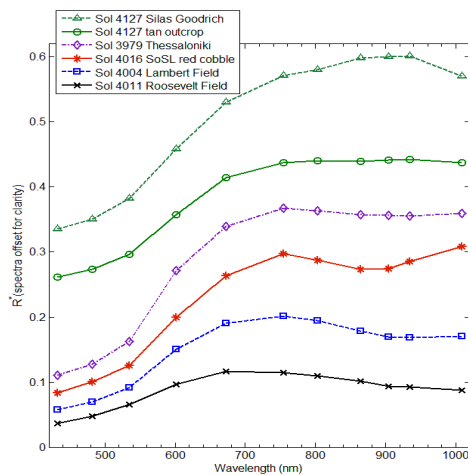


**Fig. 3.** Representative spectra of groupings represented by colors on SOM in **Fig. 2**.

**Interpretations:** The SoSL dark rocks, represented by the sol 4011 Roosevelt Field observation have a negative slope in the NIR and low 535 nm band depths consistent with rocks of basaltic compositions. The “SoSL purple rocks” grouping of **Fig. 2** includes rocks examined in SoSL including Lambert Field, Lone Eagle and H.M. Bixby. These rocks have 904 nm bands that are potentially attributable to crystalline ferric oxides and/or low-Ca pyroxenes. The Thessaloniki RAT brush also displayed evidence of a shallow NIR absorption band and elevated 535 nm band depth indicative of the presence of crystalline ferric oxide minerals. At SoSL and on the floor of Marathon Valley curvilinear “red zones” have been observed. Closer examination in SoSL at the Pvt. William Bratton target and in Marathon Valley at the Pvt. Silas Goodrich target indicated the presence of fragmented rocks with relatively strong 535 nm band depths but with a convex shape in the NIR with a steeply negative 934 to 1009 nm slope (**Fig. 3** and **Fig. 4**). As noted in [8], these rocks are elevated in Al and Si and depleted in Fe. The tan outcrop in Marathon Valley has a relatively flat NIR spectral shape. The “hematitic” grouping includes spectra of cobbles observed near the H.M. Bixby IDD target and also of patches within the “red zone” examined at SoSL (the Pvt. William Bratton target). These observations have red hematite-like spectra with a 864 nm band minimum and positive 754 to 1009 nm and 934 to

1009 nm slopes. No representatives of this grouping have been examined *in-situ* by Opportunity.

**Conclusions:** Fractures in the rim of Endeavour have indicated chemically and spectrally distinct materials from the rest of the rim [9]. The presence of ferric oxide minerals and possible hydration in the “red zones” (indicated by the negative 934 to 1009 nm slope) is consistent with aqueous alteration in these regions including SoSL and Marathon Valley.

**References:** [1] Squyres S.W. et al. (2012) *Science*, 336, 570. [2] Arvidson R.E. et al. (2014) *Science*, 343, doi:10.1126/science.1248097. [3] Bell J.F. III et al. (2006) *JGR*, 108, doi:10.1029/2003JE002070. [4] Farrand W.H. et al. (2013) *Icarus*, 225, 709. [5] Farrand W.H. et al. (2014) *JGR*, 119, doi:10.1002/2014JE004641. [6] Kohonen T. (1988) *Self-Organization & Associative Memory*, 312 pp. [7] Wehrens R. and Buydens L.M.C., *J. Stat. Softw.*, 21, 5. [8] Mittlefehldt D.W. et al. (2016) LPSC 47, submitted. [9] Farrand W.H. et al. (2015) GSA Annual Meeting, # 234-6.

**Acknowledgements:** MER work was funded via a Participating Scientist sub-contract through JPL.

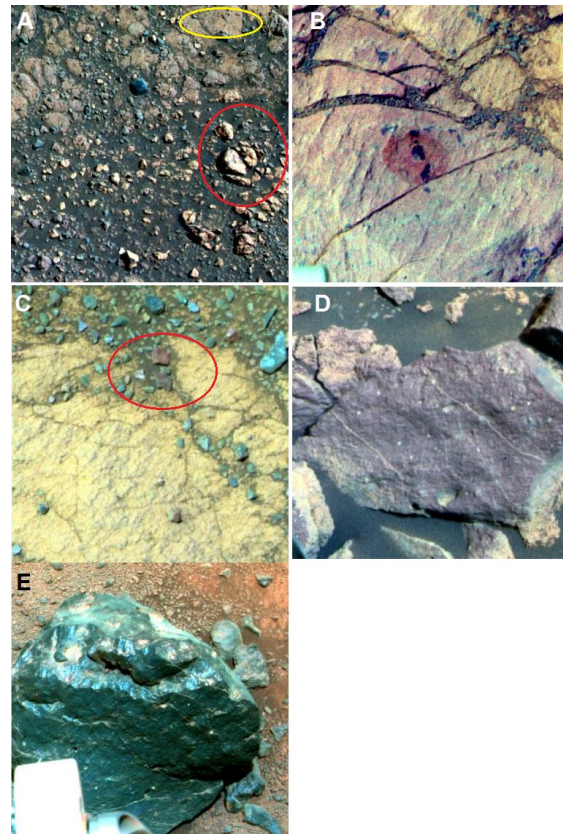


**Fig. 4.** L357 (673, 535, 432 nm composites) **A.** Sol 4127 P2440 red circle on Silas Goodrich “red zone”, yellow circle on “tan outcrop”. **B.** Sol 2530 P2530 Thessaloniki RAT brush. **C.** Sol 4016 P2553 H.M. Bixby red cobble (circled). **D.** Sol 4004 P2542 Lambert Field. **E.** Sol 4011 P2550 Roosevelt Field.